Title Page

Classifications:

Physical Sciences: Chemistry

Biological Sciences: Ion channels

Title:

Differential Effects of Modified Batrachotoxins on Voltage-gated Sodium Channel Fast and Slow Inactivation

Tim M. G. MacKenzie[1+], Fayal Abderemane-Ali[2+], Catherine E. Garrison[1+], Daniel L. Minor, Jr.[2-6]* and J. Du Bois[1]*

[+]These authors contributed equally to this work

[1]Department of Chemistry, Stanford University, Stanford, CA 94305
[2]Cardiovascular Research Institute
[3]Departments of Biochemistry and Biophysics, and Cellular and Molecular Pharmacology
[4]California Institute for Quantitative Biomedical Research
[5]Kavli Institute for Fundamental Neuroscience, University of California, San Francisco, CA 93858-2330
[6]Molecular Biophysics and Integrated Bio-imaging Division, Lawrence Berkeley National Laboratory, Berkeley, CA 94720

Author Affiliation:

Tim M. G. MacKenzie, Catherine E. Garrison, J. Du Bois
Department of Chemistry
Stanford University
337 Campus Drive
Stanford, CA 94305

Fayal Abderemane-Ali, Daniel L. Minor, Jr.
Cardiovascular Research Institute
University of California, San Francisco
Box 3122
555 Mission Bay Blvd. South, Rm. 452Z
San Francisco, CA 94158-9001

Corresponding Authors

J. Du Bois jdubois@stanford.edu
Daniel L. Minor, Jr. daniel.minor@ucsf.edu

Author contributions:

T.M.G.M and J.D. originally conceived of the project. T.M.G.M, F.A.A., and C.E.G. performed research; all authors were involved in analyzing the data. T.M.G.M and J.D. wrote the paper with input from C.E.G, F.A.A, and D.L.M.

Disclosure

J.D. is a cofounder and holds equity shares in SiteOne Therapeutics, Inc., a start-up company interested in developing subtype-selective modulators of Na_V.

Keywords: Sodium channel, batrachotoxin, Site II, electrophysiology, inactivation

Text

Abstract:

Voltage-gated sodium channels (Na_Vs), large transmembrane protein complexes responsible for the initiation and propagation of action potentials, are targets for a number of acute poisons. Many of these agents act as allosteric modulators of channel activity and serve as powerful chemical tools for understanding channel function. Batrachotoxin (BTX) is a steroidal amine derivative most commonly associated with poison dart frogs and is unique as a Na_V ligand in that it alters every property of the channel, including threshold potential of activation, inactivation, ion selectivity, and ion conduction. Structure-function studies with BTX are limited, however, by the inability to access preparative quantities of this compound from natural sources. We have addressed this problem through *de novo* synthesis of BTX, which gives access to modified toxin structures. In this report, we detail electrophysiology studies of three BTX C20-ester derivatives against recombinant Na_V subtypes (rat $Na_V1.4$ and human $Na_V1.5$). Two of these compounds, BTX-B and BTX-^{c}Hx, are functionally equivalent to BTX, hyperpolarizing channel activation and blocking both fast and slow inactivation. BTX-yne—a C20-*n*-heptynoate ester—is a conspicuous outlier, eliminating fast but not slow inactivation. This unique property qualifies BTX-yne as the first reported Na_V modulator that separates inactivation processes. These findings are supported by functional studies with bacterial Na_Vs (BacNa_Vs) that lack a fast inactivation gate. The availability of BTX-yne should advance future efforts aimed at understanding Na_V gating mechanisms and designing allosteric regulators of Na_V activity.

Significance Statement:

Voltage-gated sodium ion channels (Na_Vs) are obligatory protein complexes for generating electrical signals in neuronal cells. These molecular machines operate through complex mechanisms in order to regulate the flow of sodium ions across cellular membranes. Understanding how Na_Vs function and how small molecules that target these channels modulate ion conduction will inform efforts in pharmaceutical research to design precision therapeutics for treating Na_V-related pathologies.

\body

INTRODUCTION

Voltage-gated sodium channels (Na_Vs) are central to physiological function as requisite protein complexes that drive the initiation and propagation of action potentials in electrically excitable cells.[1] Na_V malfunction underlies a number of human pathologies and, unsurprisingly, acute disruption of Na_V activity can be fatal.[2] A large and structurally disparate collection of poisons occur in Nature that target Na_Vs.[3] The lethality of these agents notwithstanding, peptide and small molecule toxins have proven invaluable as chemical reagents for studies of Na_V structure and dynamics. Among such molecules, one natural product—batrachotoxin (BTX)—is conspicuous. BTX is a steroidal amine derivative commonly associated with poison dart frogs, but also found in species of bird and beetle.[4,5] This toxin is unique among all other Na_V modulators in that it affects every measurable aspect of Na_V function including activation threshold, inactivation, single channel conductance, and ion selectivity.[4b,6] Because of its chemical complexity and lack of availability from natural sources, studies to dissect how the different structural elements of BTX contribute to altering channel function are limited.[7,8] *De novo* synthesis, however, has enabled access to (–)-BTX and modified forms thereof.[9] In this report, experiments comparing the effects of BTX and three BTX C20-ester derivatives against skeletal muscle and cardiac Na_Vs reveal a singular agent, BTX-yne, that differentially influences fast and slow channel inactivation. This unique property distinguishes BTX-yne as a powerful new tool for biophysical and pharmacological studies of Na_Vs. The availability of BTX-yne should advance efforts to understand the mechanisms underlying Na_V gating and guide the development of allosteric modulators for treating Na_V-related disorders.

BACKGROUND

Eukaryotic Na_Vs are heteromeric protein complexes consisting of a pore forming α-subunit and up to two auxiliary β-proteins.[1a,3c,10] The α-subunit, of which there are nine different isoforms ($Na_V1.1$–1.9), derives from a single polypeptide chain that clusters into four homologous repeats (DI–DIV), each consisting of six transmembrane α-helices (S1–S6). Functionally, Na_Vs have two 'gates' (activation and inactivation gates), both of which must be open in order for ion conduction to occur.[11]

The simplest model to describe Na_V gating posits three limiting conformations: 1) a non-conducting closed state that is primed to respond to membrane depolarization; 2) an open, conducting state; and 3) a non-conducting inactivated state.[12] Inactivated channels must transition back to a closed form before firing again. A sufficiently strong membrane depolarization induces the outward movement of the voltage-sensors, causing channels to open (activation). Opening is rapidly followed by inactivation, which occurs on the millisecond time scale (fast inactivation). Fast inactivation involves the movement of a hydrophobic IFM motif located on a loop connecting DIII-DIV, which allosterically effects pore closure.[13,14] An alternative form of Na_V inactivation (slow inactivation) takes place over longer time scales (seconds to minutes) and results from repetitive or sustained membrane depolarization.[15] Additionally, channels can directly inactivate from the closed state without ever entering the open state (closed-state inactivation).[16] The steady-state distribution of closed, open, and inactivated channels at a resting membrane potential is intrinsic to each Na_V α-subunit. Natural toxins and other small molecules that bind the α-subunit are generally biased toward a particular conformational state of the channel and can affect one or more properties such as ion conduction, channel activation, inactivation, and ion selectivity.[3,17] Studies with such agents have been instrumental in dissecting the complex dynamics of channel gating.

Among the most venerable Na_V toxins is the steroidal derivative, batrachotoxin (BTX), the active component in poison darts obtained from frog secretions by Colombian natives.[18] BTX is the prototypical

member of the family of lipid soluble toxins that lodge in the inner pore of the channel (termed Site II). These toxins are unique in simultaneously binding to the inner pore and disrupting channel gating. Notably, BTX binding affects every measurable aspect of Na_V function: the activation threshold is shifted in the hyperpolarizing direction by 30–50 mV, both fast and slow inactivation are abolished, single channel conductance is reduced, and ion selectivity is compromised.[6a,b,19] Efforts to understand BTX activity have relied on electrophysiology in combination with protein mutagenesis and structure-activity relationship (SAR) studies.[6b,20] Ligand docking studies with homology models of the Na_V pore suggest specific contacts between toxin and channel but, to date, reveal little about toxin function. The studies detailed herein are enabled by our ability to access BTX through a multistep synthesis.[9] This work has led to the identification of a novel BTX derivative, BTX-yne, which alters Na_V gating by inhibiting fast, but not slow, inactivation. This characteristic is distinct from BTX and two other C20-ester variants, all three of which block both fast and slow inactivation. To our knowledge, no other small molecule or peptide that separates these two functional features of the channel has been described.

RESULTS

Synthesis of BTX derivatives. Following our reported synthesis of batrachotoxinin A (BTX-A), we have optimized conditions for modifying the C20 alcohol in order to install different ester groups (**Scheme 1**). The ester moiety is essential for toxin activity, as BTX-A is >1,000 times less potent than the parent compound.[4b,21] For the purpose of this study, four compounds were prepared, BTX, BTX-B, BTX-^{c}Hx, and BTX-yne, and evaluated against recombinant rat skeletal muscle sodium channels (rNa_V1.4). The benzoate ester, BTX-B, has been reported previously, and is generally regarded as a functional equivalent of BTX;[6c,7a] however, a direct quantitative comparison of BTX and BTX-B compounds has not been detailed. The other two derivatives, BTX-^{c}Hx and BTX-yne, were designed to assess the importance of the aryl moiety for toxin activity against Na_V.[20g,22] We note that BTX-yne and BTX-^{c}Hx were selected over other ester groups, as these two derivatives are comparable to BTX and BTX-B in terms of lipophilicity based on similar cLogP values (BTX 3.22; BTX-B 4.12; BTX-yne 3.58; BTX-^{c}Hx 4.47).[23]

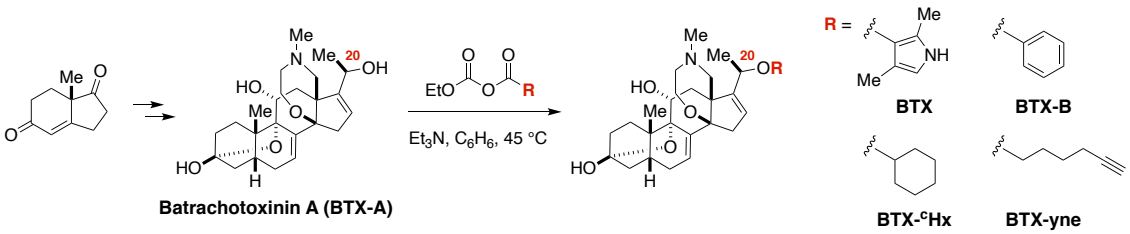

Scheme 1. Synthetic route to BTX C20-ester derivatives.

Functional characterization of BTX and BTX derivatives on Na_V activity. Whole cell voltage-clamp electrophysiology recordings were performed to assay the effects of BTX, along with the other three ester derivatives, against rNa_V1.4 transiently expressed in Chinese hamster ovary (CHO) cells. For initial characterization studies, we evaluated all four compounds using the same voltage stimulation protocol. Because BTX is known to preferentially interact with the open state of Na_Vs, cells treated with toxin were stimulated with 2000 step pulses from –100 mV to 0 mV at 2 Hz frequency to promote toxin access to the receptor site.[24] Na_V response to a step depolarization to 0 mV in the absence and presence of BTX is shown in **Figure 1A**. In contrast to unmodified channels, which quickly reach a peak current and then completely inactivate within 2–3 milliseconds, toxin-modified channels remain open throughout the duration of the step pulse. A large tail current is observed upon hyperpolarization to –100 mV (**Figures 1A and S1E**). Channels treated with BTX-B and BTX-^{c}Hx present similar current traces (**Figure S1M and S1U**). By contrast, BTX-yne-modified channels show a marked

reduction in the rate of deactivation (**Figures 1B and S1CC**), suggesting that BTX-yne is more effective than the other three compounds at stabilizing the open state.

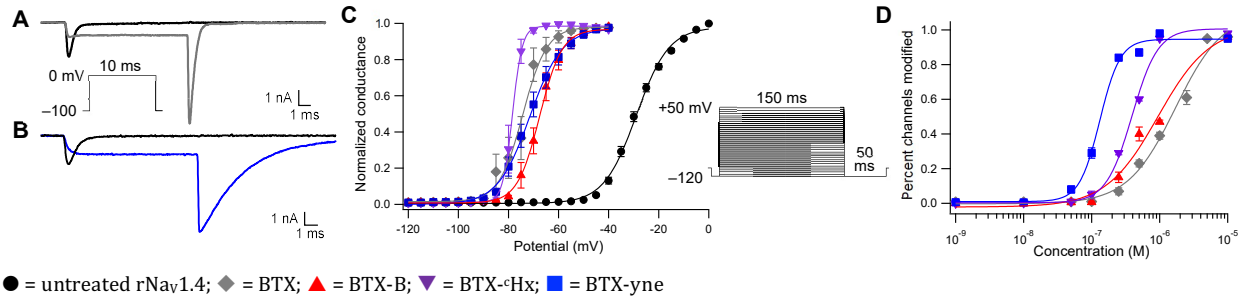

Figure 1. (A) Representative trace for $Na_V1.4$ current before (black) and after (grey) steady-state binding of 10 μM BTX. Current was evoked by a 10-ms test pulse from –100 to 0 mV after establishment of steady-state activity by repetitive depolarizing pulses to 0 mV. Inset: step-depolarization to elicit current response. (B) Representative trace for $Na_V1.4$ current before (black) and after (blue) steady-state binding of 5 μM BTX-yne. Current was evoked by a 10-ms test pulse from –100 to 0 mV after establishment of steady-state activity by repetitive depolarizing pulses to 0 mV. (C) Voltage-dependence of activation before (black circles) and after application of 10 μM toxin to CHO cells expressing $Na_V1.4$. Inset: stimulation protocol for measuring voltage-dependence of channel activation. Normalized conductance was plotted against the recording potential and fit with a sigmoid function; data represent n ≥ 3 ± SEM. Black circles = no compound, grey diamonds = BTX, red triangles = BTX-B, purple inverted triangles = BTX-^{c}Hx, blue squares = BTX-yne. (D) Concentration-response curve for activation of $Na_V1.4$ by BTX and derivatives (n ≥ 3 ± SEM).

Application of BTX to $Na_V1.4$ has a pronounced influence on the threshold potential at which channels open, shifting the half-activation potential ($V_{½\ act}$) by −45 mV. Using the same multistep activation protocol, we measured the influence of BTX derivatives (10 μM) on this value (**Figures 1C, S1**). The resulting activation curves show that all three derivatives have effects similar to BTX on threshold activation, albeit with small differences in the slope factors (k) (**Figure 1C, Table 1**). Activation curves obtained at a sub-saturating concentration of toxin were fitted by a sum of two Boltzmann equations, revealing two populations of channels: 1) toxin-modified channels with more negative $V_{1/2\ act}$ values; and 2) unmodified channels with typical $Na_V1.4$ $V_{½\ act}$ values of −30 mV (**Figure S1, Table S1**). At 100 nM toxin, the extent to which channel activation is altered differs between the four compounds (**Figure S1; Table S1**). To determine EC_{50} values, the effect of toxin at different concentrations on channel activation was measured (**Figures 1D, S2**). Based on this analysis, BTX-yne is the most potent compound with an EC_{50} that is ~16 times lower than BTX itself.

Table 1. Boltzmann fit and affinity parameters for untreated and toxin-modified $rNa_V1.4$

Toxin	$V_{1/2\ act}$ (mV)	$\Delta V_{1/2\ act}$ (mV)	*k* (mv)	EC_{50} (nM)	EC_{50} (from SSI)
none	–28.9 ± 0.3	–	6.5 ± 0.3	–	–
BTX	–74.3 ± 0.6	–45.4 ± 0.7	4.8 ± 0.5	2074 ± 768	2237 ± 1120
BTX-B	–67.5 ± 0.2	–38.6 ± 0.4	4.5 ± 0.2	756 ± 43	795 ± 113
BTX-^{c}Hx	–78.4 ± 0.1	–49.5 ± 0.3	2.0 ± 0.1	491 ± 26	494 ± 37
BTX-yne	–71.4 ± 0.3	–42.7 ± 0.4	6.5 ± 0.3	130 ± 21	189 ± 59

The relative potencies of BTX and BTX derivatives against $Na_V1.4$ can be further assessed by considering either the ratio of sustained current/peak current or the ratio of tail current/peak current resulting from a strong depolarization.[20e,h] We evaluated the four toxins in both ways and found toxin activities to mirror EC_{50} data (**Figures 2D and S2, Table S2**). Our findings validate and demonstrate the equivalency of such protocols for quantitatively analyzing the action of these compounds.

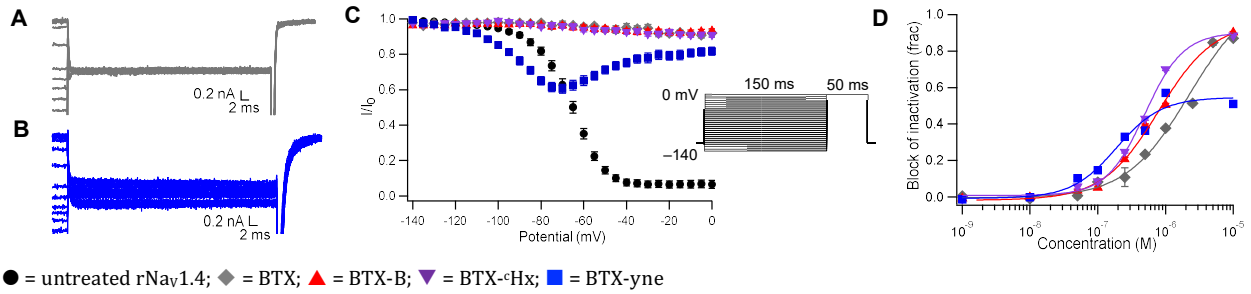

Figure 2. (A) Representative trace for $Na_V1.4$ current after (grey) steady-state binding of 10 μM BTX during the test pulse of the inactivation protocol (C, inset). Current was evoked by a 50-ms test pulse from –100 to 0 mV after establishment of steady-state activity by repetitive depolarizing pulses to 0 mV and following a variable conditioning pulse. (B) Representative trace for $Na_V1.4$ current after (blue) steady-state binding of 5 μM BTX-yne using the same inactivation protocol as in (A). (C) Voltage-dependence of inactivation before (black circles) and after application of 10 μM of the indicated toxin to CHO cells expressing $Na_V1.4$. Data were recorded using the stimulation protocol shown in Figure 2C inset. Normalized current (I/I_0) in the test pulse was plotted against the conditioning potential; data represent n ≥ 3 ± SEM. Black circles = no compound, grey diamonds = BTX, red triangles = BTX-B, purple inverted triangles = BTX-^{c}Hx, blue squares = BTX-yne. (D) Concentration-response curve for block of inactivation of $Na_V1.4$ by BTX and derivatives (n ≥ 3 ± SEM).

BTX derivatives differentially influence Na_V inactivation. A signature effect of BTX on Na_V activity is the elimination of both fast and slow inactivation (**Figure 1A**). To determine if C20-ester substitution of the toxin alters this behavior, we used a two-pulse protocol to measure steady-state inactivation, SSI (**Figure 2 inset**).[25] Channels that inactivate in the pre-pulse period are unavailable to open in the test pulse. A plot of normalized current versus voltage (I/I_o–V) for unmodified channels (black circles) under this SSI protocol is shown in **Figure 2C**. Analogous SSI curves for toxin-treated Na_Vs display similar Boltzmann behavior, but a fraction of the total population of channels is non-inactivating; this percentage varies in a dose-dependent manner (**Figure S3, Table S3**). At saturating concentrations of BTX, BTX-B, and BTX-^{c}Hx, inactivation is completely abrogated (**Figures 2A, S3**). EC_{50} values for the SSI response were determined by varying toxin concentration, (**Table 1**). These values accord with voltage of activation EC_{50}s for each compound.

Comparison of SSI curves recorded at saturating concentration (10 μM) of each of the four toxin derivatives reveals an unexpected difference for BTX-yne (**Figures 2A-C, S3**). In contrast to BTX, BTX-B, and BTX-^{c}Hx, which eliminate inactivation, BTX-yne-modified channels are able to inactivate partially. Interestingly, a plot of I/I_0 versus voltage appears as a U-shaped SSI curve (*vide infra*). The extent to which BTX-yne-treated channels are inactivated can be estimated by applying a baseline correction to the SSI curve (**Figure S4**). From this analysis, 40–50% of channel inactivation occurs at a saturating concentration of BTX-yne as compared to ca. 100% and 0% for untreated and BTX-B-modified channels, respectively. The influence of BTX-yne on SSI is not unique to $rNa_V1.4$, as $hNa_V1.5$ channels treated with this compound (5 μM) are similarly altered (**Figure S5**).

Although all four toxin derivatives shift the activation voltage dependence to a comparable extent, BTX-yne stands alone as the only compound that does not completely inhibit channel inactivation (**Figures 1C and 2C**). Superposition of the voltage-dependent activation and inactivation curves shows that, in presence of BTX-yne, inactivation initiates at potentials at which channels are closed (< –100 mV) and persists even when all channels are open (> –40 mV) (**Figure S4E-F**). This observation suggests that BTX-yne-modified channels undergo inactivation from both the closed and open states (i.e., closed-state and open-state inactivation, respectively). Recording data shown in **Figure 1B** illustrate that BTX-yne blocks $Na_V1.4$ fast inactivation, analogous to the other three agents (**Figure S3**). The question thus arises, can BTX-yne-modified channels transition to a non-conducting state through slow inactivation? To address this question, we first determined the time constant for BTX-yne-modified channels to undergo slow inactivation at –70 mV. This potential was chosen as it

represents the lowest point of the U-shaped SSI curve (i.e., the point at which maximum inactivation is evident in the raw current recording).

Cells were stepped from a holding potential of –120 mV to –70 mV for varying lengths of time, Δt. Following this conditioning pulse, the extent to which channels inactivate as a function of Δt was measured in a test pulse to 0 mV (**Figure S6**.[26] BTX-B was employed as a negative control for these experiments, as channels bound to this compound remain conducting irrespective of the time period of the conditioning or test pulses. Using this stimulation protocol, cells treated with 10 μM BTX-yne display a clear exponential decay of peak current as a function of the conditioning pulse length. Fitting these data for BTX-yne to two exponentials gives a time constant, τ, for each process (τ_{fast} = 90.8 ± 3.8 ms; τ_{slow} = 929.9 ± 325.1 ms). Accordingly, a stimulation protocol to measure slow-inactivation of BTX-yne-modified channels requires conditioning pulses >> 1000 ms in duration to ensure that equilibrium is achieved between successive current recordings.

The effect of each toxin on slow inactivation was examined using the stimulation protocol shown in **Figure 3 (inset)**. A conditioning pulse was applied from –140 mV to 0 mV in 5 mV increments over a 6,500 ms interval (6.5 x τ_{slow}). Following the pre-pulse, a 150 ms test pulse to 0 mV measured channel availability. In unmodified channels, a brief hyperpolarizing step (10 ms) to –120 mV was included to recover from fast inactivation (not shown in **Figure 3A**, see **Figure S7**). The addition of this step pulse is both unnecessary and problematic in recordings of toxin-modified channels—the former because all four compounds block fast inactivation, the latter stemming from the large and variable tail currents, which interfere with measurements in the test pulse.

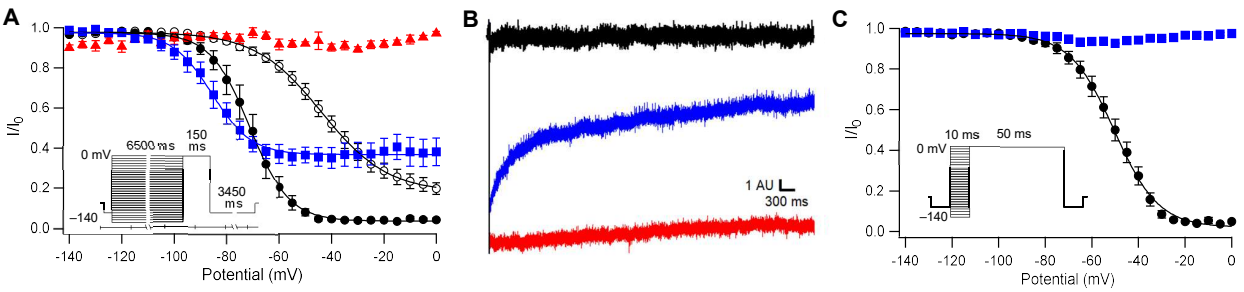

Figure 3. (A) Voltage-dependence of slow inactivation before (black circles) and after application of 10 μM BTX-B (red triangles) or BTX-yne (blue squares). Inset: stimulation protocol for measuring voltage dependence of slow inactivation (note the truncated x-axis). Normalized current in the test pulse was plotted against the conditioning potential and fit with a sigmoid function; data represent n ≥ 3 ± SEM. Open circles represent unmodified channels recorded with a hyperpolarizing step after the conditioning pulse to account for fast-inactivated channels; see Figure S7 for details. (B) Representative trace for $Na_V1.4$ current before (black) and following application of 10 μM BTX-B (red) or BTX-yne (blue). Current was evoked by a 6,500-ms test pulse from –100 to 0 mV after steady-state was obtained through repetitive depolarizing pulses to 0 mV. Note that the y-axis units are arbitrary as the peak current for each trace has been normalized to the same magnitude. (C) Voltage-dependence of fast inactivation before (black circles) and following application of 10 μM BTX-yne (blue squares). Inset: stimulation protocol for measuring voltage dependence of fast inactivation. Normalized current in the test pulse was plotted against the conditioning potential and fit with a sigmoid function; data represent n ≥ 3 ± SEM.

Using the protocol shown in **Figure 3A** (inset), absent a hyperpolarizing step to recover from fast inactivation, the inactivation response of unmodified channels (black circles) displays sigmoidal behavior (**Figure 3A**). When a 10 ms hyperpolarizing step to –120 mV is included to enable channels to recover from fast inactivation, the voltage-dependence of SSI is shallower (i.e., larger k value) and shifted considerably to higher potential, and normalized current (I/I_0) never reaches zero (open circles). Channels modified by 10 μM BTX-B do not inactivate in either the conditioning or the test pulse (**Figures 3A** and **3B**, red triangles), analogous to BTX.[27] By contrast, channels modified with 10 μM BTX-yne exhibit a clear voltage-dependent slow inactivation with current decaying to a steady-state

value that is ~60% of the peak current, I_0 (**Figures 3A** and **3B**, blue squares). Two principal conclusions follow from these data: 1) ~80% of unmodified channels enter a slow-inactivated state (open circles, **Figure 3C**); 2) BTX-yne-modified channels are able to undergo slow inactivation. The latter finding is in marked contrast to channels treated with BTX-B, for which both fast and slow inactivation are entirely inhibited.

To obtain additional support for the above conclusions, we used an amended stimulation protocol to measure fast inactivation (**Figure 3C, inset**). In these experiments, a short conditioning pulse (10 ms) only allows time for channels to undergo fast inactivation. Accordingly, application of 10 μM BTX-yne to cells under this protocol gives no evidence of inactivation (**Figure 3C**). In fact, these data look indistinguishable from the inactivation plots of other BTX derivatives (**Figure 2B**). These results confirm that BTX-yne prevents fast inactivation and that BTX-yne-modified channels are able to access the slow-inactivated state.

BTX derivatives differentially affect bacterial Na_V inactivation. Our findings with $Na_V1.4$ and $Na_V1.5$ implicate BTX-yne as an inhibitor of fast but not slow inactivation. To interrogate further the activity of this toxin derivative, we have examined the influence of BTX-yne as well as BTX, BTX-B, and BTX-^{c}Hx on Na_Vs that lack a fast inactivation gate. Bacterial Na_Vs (BacNa_Vs) form as homotetramers of noncovalently associated domains, analogous to voltage-gated K^+ channels, and lack the DIII–DIV linker and IFM particle (or a functional equivalent) responsible for fast inactivation in eukaryotic channels.[28,29] Thus, only slow inactivation is operative in BacNa_Vs.

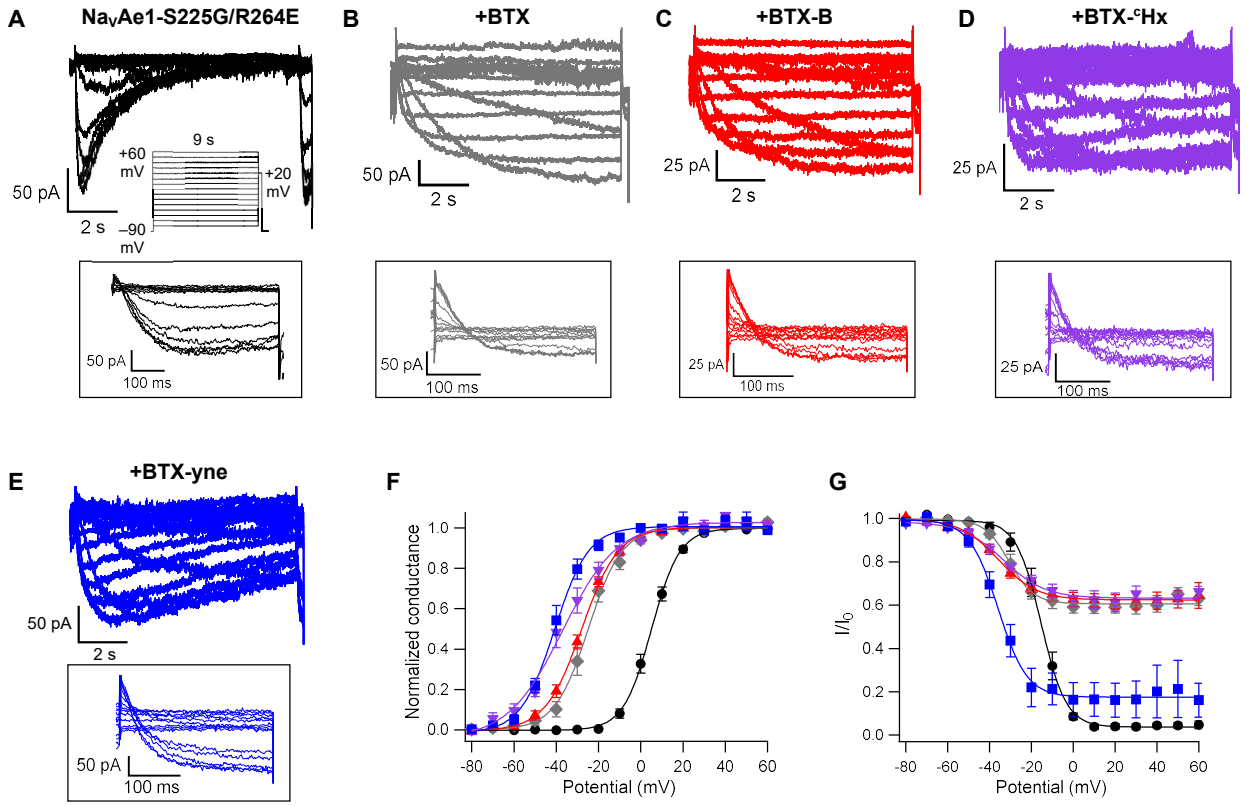

Figure 4. (A–E) Representative current recordings for NaVAe1-S225G/R264E before (A) and after application of 10 μM BTX (B), BTX-B (B), BTX-^{c}Hx (D) and BTX-yne (E), in response to an inactivation protocol (inset). Boxed traces are magnification of the current in response

to the +20-mV test pulse. (F) Activation and (G) inactivation voltage dependence for Na_VAe-S225G/R264E before (black circle) and after application of 10 μM BTX (grey diamonds), BTX-B (red triangles), BTX-^{c}Hx (purple inverted triangles) or BTX-yne (blue squares).

We initially examined Na_VBh1 (NachBac), a well-studied $BacNa_V$ that is sensitive to BTX.[30] In line with our work and previous reports of BTX activity against eukaryotic Na_Vs, toxin application (10 μM) stabilized the Na_VBh1 open state and shifted the activation voltage dependence towards hyperpolarizing potentials (**Figure S8A-B and D**). Unlike eukaryotic Na_Vs, however, Na_VBh1 proved surprisingly insensitive to BTX-B (**Figure S8C-D**). An alternative $BacNa_V$, Na_VAe1, from *Alkalilimnicola ehrlichii*[31] bearing a mutation in the cytosolic C-terminal domain 'neck region' (R264E) to enable functional studies[32] was only modestly influenced by BTX (**Figure S8E-G**). To understand these unexpected differences in toxin activity, we examined sequence alignments of the inner pore S6 helices of select bacterial and eukaryotic channels (**Figure S8H**). This analysis identified a serine residue in the Na_VAe1 inner pore that appears as a glycine in Na_VBh1 and in three of the four S6 helices in eukaryotic Na_Vs (**Figures S8H-I**). Mutation of S225 to glycine (S225G) in Na_VAe1 R264E yields a channel that is sensitive to both BTX and BTX-B (**Figures 4A-C**, **S8J-K**) as well as BTX-^{c}Hx, and BTX-yne (**Figures 4D-E**). All four compounds cause substantial hyperpolarizing shifts in activation and inhibit channel inactivation (**Figures 4A-F**). Electrophysiology recordings to measure steady-state inactivation confirm that BTX, BTX-B, and BTX-^{c}Hx block significantly inactivation of Na_VAe1 S225G-R264E (**Figures 4B-D, 4G**). In marked contrast, Na_VAe1 S225G-R264E channels exposed to BTX-yne show a strong SSI response, as noted in unmodified channels (**Figure 4G**). This result offers compelling evidence that BTX-yne, unlike the other three compounds, is ineffective at blocking inactivation in this mutant $BacNa_V$.

DISCUSSION

We have synthesized batrachotoxin and three C20-ester derivatives and characterized these compounds by whole cell electrophysiology against $rNa_V1.4$. All four compounds significantly hyperpolarize $V_{1/2}$ of activation, albeit with some variation in the magnitude of this effect (see **Table 1**). We have examined different protocols to measure the influence of non-saturating toxin concentrations on channel activity and have established that these methods give similar outputs.[20e,h] Concentration-response measurements quantify the relative activity of BTX, BTX-B, BTX-^{c}Hx, and BTX-yne. The potencies of BTX, BTX-B, and BTX-^{c}Hx, the three derivatives that eliminate fast and slow inactivation, track with cLogP values for these compounds (cLogP: 3.22, 4.12, 4.47; EC_{50} for $V_{1/2}$ activation: 2074 nM, 756 nM, 491 nM, respectively).[23] This trend is consistent with toxin binding at Site II, as the inner pore of the channel is a receptor for hydrophobic molecules. To our knowledge, this work represents the first systematic analysis of toxin potency against a recombinant Na_V subtype.

The influence of BTX on channel inactivation is pronounced, as channels remain persistently conducting, unable to conformationally rearrange in a manner that stops the flow of ions.[4] Our findings demonstrate that BTX-B and BTX-^{c}Hx, like the parent toxin, block fast and slow inactivation mechanisms. Channels modified by BTX-yne are also prevented from rapidly inactivating. BTX-yne binding, however, does not preclude channels from undergoing a slow, voltage-dependent transition to a non-conducting state. Slow inactivation is thought to involve extensive protein conformational changes, but a structural understanding of this process is still lacking.[33,34,35] Toxin derivatives such as BTX-yne should aid studies of this intriguing gating mechanism.

Additional evidence that BTX-yne is unable to block slow inactivation follows from investigations with the bacterial sodium channel mutant, Na_VAe1 S225G-R264E. As with other $BacNa_V$s, Na_VAe1 S225G-R264E lacks a fast inactivation particle and, thus, has only one mechanism for transitioning from an open to a non-conducting state. Electrophysiological recordings of Na_VAe1 S225G-R264E following treatment with BTX, BTX-B, or BTX-^{c}Hx display essentially equivalent effects in which all

three compounds induce a large hyperpolarizing shift in activation voltage dependence and block inactivation (**Figures 4B-D, 4F, 4G**). These data are similar to results with eukaryotic channels, $Na_V1.4$ and 1.5. By contrast, Na_VAe1 S225G-R264E channels modified by BTX-yne, for which activation voltage is significantly hyperpolarized, can enter a non-conducting state (**Figures 4E-G**) The inability of BTX-yne to block inactivation in Na_VAe1 S225G-R264E supports our conclusion that this same compound is incapable of blocking slow inactivation in mammalian Na_Vs.

A simplified four-state model is sufficient to appreciate the differences between BTX and BTX-yne on Na_V gating.[36] Closed channels, unmodified by toxin, can enter either an open (conductive) or slow-inactivated (non-conductive) state (**Figure 5A**). The degree to which either pathway is favored is voltage dependent. Open channels quickly become non-conducting through a mechanism of fast-inactivation and a secondary inactivation pathway that is kinetically slower. BTX, as well as BTX-B and BTX-^{c}Hx, facilitate the closed→open transition and block both inactivation processes; thus, channels open upon membrane depolarization at more negative potentials and remain conductive.

As with BTX, BTX-yne influences the steady-state population of closed*⇆open* channels and inhibits fast-inactivation (note: * reflects BTX-yne-bound channels, **Figure 5B**). Channel inactivation, however, through closed*⇆slow inactivated* (i.e., closed-state inactivation) and open*⇆slow inactivated* transitions is not blocked by BTX-yne. The combination of: 1) inhibition of fast inactivation and 2) slow conversion from the open*→slow-inactivated* state relative to the time duration of the conditioning pulse (150 ms) in the SSI protocol give rise to the unusual U-shaped SSI curve for BTX-yne-modified Na_Vs (see **Figure 2B**). As conditioning pulses in the SSI protocol are stepped to higher depolarizing potentials, the fraction of channels transitioning from closed*→slow-inactivated* first increases in a voltage-dependent manner, leading to the downstroke of the current versus voltage response, which reaches a nadir at –70 mV. Conditioning depolarizations > –70 mV result in fewer channels undergoing closed-state inactivation, leaving a larger number of channels available to activate. Open* channels cannot fast inactivate and do not have sufficient time to slow inactivate* given the 150 ms duration of the conditioning pulse (recall that τ_{slow} = 930 ms, **Figure S6**). As such, an increase in current is measured at higher step potentials (the upstroke of the U-shaped curve). This interpretation is consistent with the absence of U-shaped SSI curve for BTX-yne-modified Na_Vs with longer (6500 ms) conditioning pulses (**Figure 3A**).

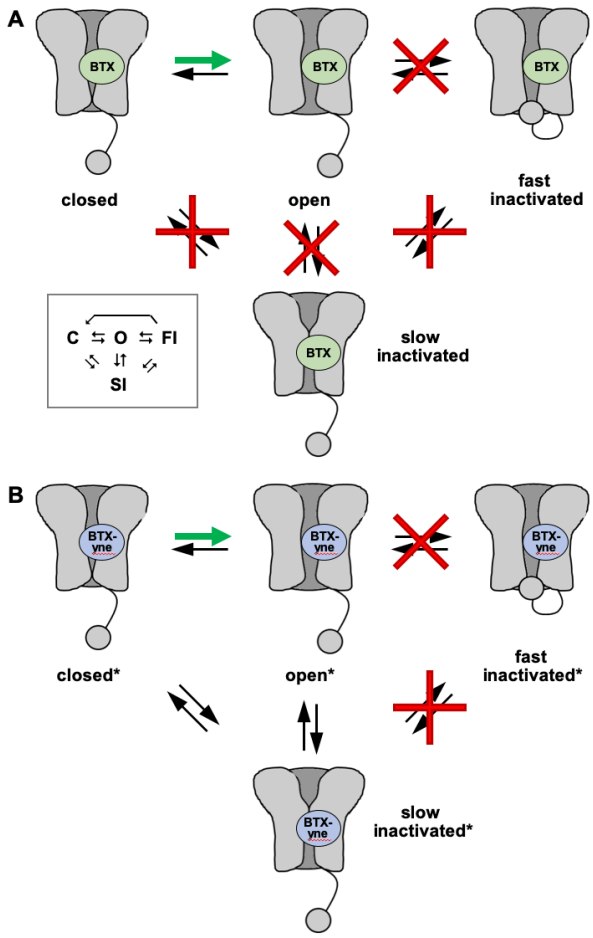

Figure 5. A simplified schematic diagram detailing the influence of toxin binding on the transitions between limiting Na_V conformational states. (a) Inset: four-state gating model for unmodified Na_V (C = closed, O = open, FI = fast-inactivated; SI = slow-inactivated); BTX (and BTX-B, BTX-^{c}Hx) facilitates the C→O transition (green arrow) and blocks both fast and slow inactivation. (b) BTX-yne facilitates the C→O transition (green arrow) and blocks fast inactivation; modified channels can transition from closed* and open* to a slow-inactivated* state.

For a derivative of BTX to function equivalently to the natural product, the full pentacyclic steroidal core as well as an ester substituent at C20 are necessary. Studies with semi-synthetic BTX derivatives demonstrate that removal of the C20-ester results in compounds that lose considerable potency (**Figure S9**.[37] Reduction of the B-ring double bond in BTX affords a toxin derivative that hyperpolarizes $V_{1/2}$, but no longer completely blocks inactivation. Synthetic analogues of the AB-ring of BTX containing pendant amine groups antagonize BTX binding, but do not hyperpolarize $V_{1/2}$ or eliminate inactivation.[38] Additionally, analogues of the CDE-ring of BTX act as reversible Na_V inhibitors despite binding in the inner pore of the channel.[39] Like these compounds, the enantiomer of BTX also functions as a channel antagonist with a binding site that overlaps that of the natural product.[9]

Collectively, our findings reveal that the intrinsic rigidity of BTX, including the heteroaryl C20-ester substituent, is critical to agonist function. Modified forms of the toxin that have additional degrees of flexibility (e.g., reduced B-ring double bond, CDE-ring analogues, C20-hexynoate ester) may adopt binding poses that either block ion conduction or enable the channel to enter a partially inactivated conformational state. BTX-yne is the first small molecule tool compound that selectively eliminates Na_V fast, but not slow, inactivation. Such a reagent should enable research efforts to explore channel dynamics and the mechanism of this latter process.

CONCLUSION

Our studies to examine structure-activity relationships of BTX and a small collection of ester-modified toxins reveal the complex allosteric properties of these ligands on Na_V function. This work provides a complete electrophysiological characterization of toxin affinity and the effects of toxin binding on both channel activation and inactivation. We have identified a BTX ester derivative, BTX-yne, which affects fast and slow inactivation processes in a manner that is differential from BTX and from any other small molecule or protein toxin modulator of Na_Vs. Future studies will aim to shed light on the molecular details of BTX and BTX-yne binding to the channel. Such insights are expected to inform the rational design of small molecule Na_V modulators that offer precise control of gating.

MATERIAL and METHODS

Cell culture and electrophysiology. Electrophysiology experiments were conducted using Chinese hamster ovary (CHO) cells transiently expressing the α-subunit of rat $Na_V1.4$ ($rNa_V1.4$) or human $Na_V1.5$ ($hNa_V1.5$). CHO cell culture was prepared as described previously.[40] Briefly, cells were grown in DMEM (GIBCO, Grand Island, NY) supplemented with 10% cosmic calf serum (HyClone, Logan, UT) and 5 U/mL penicillin/streptomycin (GIBCO). Cells were kept in a 5% carbon dioxide, 96% relative humidity incubator and passaged every ~3 days. Passaging of cells was accomplished by aspiration of media, washing with phosphate-buffered saline, treatment with 1 mL trypsin-EDTA (0.05%, Invitrogen, Carlsbad, CA) for ~5 min until full dissociation of cells from the plate surface was observed and dilution with 4 mL of growth medium. Approximately 250 μL of this suspension was then diluted in 10 mL of growth medium in a new 10 cm plate. Transfection with a pZem228 vector containing the full-length cDNA coding for the α-subunit of $rNa_V1.4$ was accomplished using the calcium phosphate precipitation method. Transfection with a vector containing the full-length cDNA coding for the α-subunit of $hNa_V1.5$ was accomplished using Lipofectamine LTX. Cotransfection with EGFP was employed so that fluorescence of EGFP could be used as a marker of transfection efficiency.

Sodium currents were measured using the patch-clamp technique in the whole-cell configuration with an Axopatch-200b amplifier (Axon Instruments, Union City, CA), as previously described by Moran and coworkers.[41]
Borosilicate glass micropipettes (Sutter Instruments, Novato, CA) were fire-polished to a tip diameter yielding a resistance of 1.2-4.5 MΩ in the working solutions. The micropipette was filled with 40 mM NaF, 1 mM EDTA, 20 mM HEPESm 125 mM CsCl. The external Solution had the following composition: 160 mM NaCl, 2 mM $CaCl_2$, 20 mM HEPES. The pH of the solutions was adjusted to pH 7.4 with 50 wt% aqueous CsOH. BTX derivatives were quantified by ^{1}H NMR spectroscopy on a 600 MHz Varian Inova spectrometer. 1,3-benzodioxole was employed as an internal standard. Spectra were acquired with a relaxation delay time (d1) of 20 s and an acquisition time (at) of 10 s. Quantitation was determined by comparison of the integrations for the toxin and the internal standard of a known concentration. Toxin stock solutions prepared in dimethylsulfoxide (4 mM) were kept at –20 ºC and diluted with external solution before recording.

The output of the patch-clamp amplifier was filtered with a built-in low-pass, four-pole Bessel filter having a cutoff frequency of 10 kHz and sampled at 100 kHz. The membrane was kept at a holding potential of –100 mV. Pulse stimulation and data acquisition used 16-bit D-A and A-D converters (Axon Instruments Digidata 1322A) controlled with the pClamp software (Axon Instruments). Leak currents were subtracted using a standard P/4 protocol of the same polarity. Access resistance was always <4 MΩ and the cell capacitance was between 4 and 20 pF, as measured by the compensating circuit of the feedback amplifier. Peak were generally between 1 and 5 nA. The series resistance was typically compensated 80%. All measurements were done at ambient temperature (20-22 ºC). Recordings were made at least 5 min after establishing the whole-cell and voltage-clamp configuration to allow for stabilization of the voltage-dependent properties of the channels. Data were analyzed using custom software developed in the Igor environment (Wavemetrics). Fit of data is presented as mean ± SD. All experiments are presented as mean ± SEM for $n \geq 3$ independent measurements.

Cells were modified by toxin after stabilization of whole-cell voltage parameters and control measurements. 0.5 mL of toxin solution was applied over 60 s. Toxin binding was promoted via 2,000 pulses to 0 mV from a hold potential of –100 mV (2 Hz cycling) before measurements were performed.

Supporting Information
The Supporting Information is available free of charge on the ACS Publications website at DOI:

Experimental procedures and characterization data for BTX derivatives, electrophysiology recording data

Acknowledgments. Partial support of this work has come from the National Institutes of Health (R01 NS045684) and from a generous gift from Amgen, Inc. TMGM was supported by a fellowship from the Center for Molecular Analysis and Design (CMAD) at Stanford University. CEG is grateful for support from the Stanford ChEM-H Chemistry/Biology Interface Predoctoral Training Grant Program and the NIGMS of the NIH under Award Number T32GM120007 and to Abbott Laboratories for a Stanford Graduate Fellowship. This work was supported by grants NIH-NHLBI R01-

HL080050 and NIH-NIDCD R01-DC007664 to D.L.M., and an American Heart Association postdoctoral fellowship to F.A.-A.

REFERENCES

1. (a) *Voltage Gated Sodium Channels: Structure, Function and Channelopathies*, Handbook of Experimental Pharmacology 246, Chahine, M., Ed., Springer-Verlag, Berlin, 2018. (b) C.H. Peters, P.C. Reuben, *Voltage Gated Sodium Channels*, Handbook of Experimental Pharmacology 221, Reuben, P. C., Ed., Springer-Verlag, Berlin, 2014. (c) S. Dib-Hajj, T. Priestly, *Ion Channels: From Structure to Function* 2nd Ed., Kew, J.N.C., Davies, C.H., Eds., Oxford University Press, Oxford, 2010, pgs. 131-169. (d) B. Hille, *Ion Channels of Excitable Membranes* (Sinauer Associates, Inc., Sunderland, MA, 2001).
2. (a) F.M. Ashcroft, *Ion Channels and Disease* (Academic Press, San Diego, CA, 2000). (b) A. Lampert, A.O. O'Reilly, P. Reeh, and A. Leffler, Sodium channelopathies and pain. *Pflugers Arch.* **2010**, *460*, 249-263. (c) W.A. Catterall, S. Dib-Hajj, M.H. Meisler, D. Pietrobon, Inherited neuronal ion channelopathies: New windows on complex neurological diseases. *J. Neurosci*. **2008**, *28*, 11768-11777. (d) J.L. Fiske, V.P. Fomin, M.L. Brown, R.L. Duncan, and R.A. Sikes, Voltage-sensitive ion channels and cancer. *Cancer. Metastasis Rev.* **2006**, *25*, 493-500. (e) A.L. George Jr., Inherited disorders of voltage-gated sodium channels. *J. Clin. Invest.* **2005**, *115*, 1990-1999.
3. (a) A.L. Lukowski, A.R.H. Narayan, Natural Voltage-Gated Sodium Channel Ligands: Biosynthesis and Biology. *ChemBioChem* **2019**, *20*, 1231-1241. (b) J.R. Deuis, A. Mueller, M.R. Israel, I. Vetter, The pharmacology of voltage-gated sodium channel activators. *Neuropharmacol.* **2017**, *127*, 87-108. (c) C.A. Ahern, J. Payandeh, F. Bosmans, B. Chanda, The hitchhiker's guide to the voltage-gated sodium channel galaxy. *J. Gen. Physiol.*, **2016**, *147*, 1-24. (d) J. Kalia, M. Milescu, J. Salvatierra, J. Wagner, J.K. Klint, G.F. King, B.M. Olivera, F. Bosmans, From Foe to Friend: Using Animal Toxins to Investigate Ion Channel Function. *J. Mol. Biol.* **2015**, *427*, 158-175. (e) M. Stevens, S. Peigneur, J. Tytgat, Neurotoxins and their binding areas on voltage-gated sodium channels. *Front. Pharmacol.* **2011,** *2*:71.
4. (a) B.I. Khodorov, Batrachotoxin as a Tool to Study Voltage-Sensitive Sodium Channels of Excitable Membranes. *Prog. Biophys. Molec. Biol.* **1985**, *45*, 57-148. (b) G.B. Brown, Batrachotoxin: A Window on the Allosteric Nature of the Voltage-Sensitive Sodium Channel. *Int. Rev. Neurobiol.* **1988**, *29*, 77-116.
5. (a) J.P. Dumbacher, T.F. Spande, J.W. Daly, Batrachotoxin Alkaloids from Passerine Birds: A Second Toxic Bird Genus (Ifrita kowaldi) from New Guinea. *Proc. Nat. Acad. Sci. USA* **2000**, *97*, 12970-12975. (b) J.P. Dumbacher, A. Wako, S.R. Derrickson, A. Samuelson, T.F. Spande, J.W. Daly, Melyrid Beetles (Choresine): A Putative Source for the Batrachotoxin Alkaloids Found in Poison-Dart Frogs and Toxic Passerine Birds. *Proc. Nat. Acad. Sci. USA* **2004**, *101*, 15857-15860.
6. (a) F. Bosmans, C. Maertens, F. Verdonck, J. Tytgat, The Poison Dart Frog's Batrachotoxin Modulates $Na_V1.8$. *FEBS Lett.* **2004**, *5*, 245-248. (b) N.J. Linford, A.R. Cantrell, Y. Qu, T. Scheuer, W.A Catterall, Interaction of Batrachotoxin with the Local Anesthetic Receptor Site in Transmembrane Segment IVS6 of the Voltage-Gated Sodium Channel. *Proc. Natl. Acad. Sci. USA* **1998**, *95*, 13947-13952. (c) W.A. Catterall, C.S. Morrow, J.W. Daly, G.B. Brown, Binding of Batrachotoxinin A 20-α-Benzoate to a Receptor Site Associated with Sodium Channels in Synaptic Nerve Ending Particles. *J. Biol. Chem.* **1981**, *256*, 8922-8927.

7. (a) G.B. Brown, S.C. Tieszen, J.W. Daly, J.E. Warnick, E.X. Albuquerque, Batrachotoxinin-A 20-α-Benzoate: A New Radioactive Ligand for Voltage Sensitive Sodium Channels. *Cell. Mol. Neurobiol.* **1981**, *1*, 19-40. (b) B.I. Khodorov, E.A. Yelin, L.D. Zaborovskaya, M.Z. Maksudov, O.B. Tikhomirova, V.N. Leonov, Comparative Analysis of the Effects of Synthetic Derivatives of Batrachotoxin on Sodium Currents in Frog Node of Ranvier. *Cell. Mol. Neurobiol.* **1992**, *12*, 59-81. (c) E. Yelin, V. Leonov, O. Tikhomirova, I. Torgov, Synthesis of Steroidal Alkaloids Active on Na^+ Channels. In *Toxin as Tools in Neurochemistry.* F. Hucho, Y. A. Ovchinikov, Eds., Berlin, New York, 1983, pp. 25-33.

8. H.M. Garraffo, T.F. Spande, Discovery of Batrachotoxin: The Launch of the Frog Alkaloid Program at NIH. *Heterocycles* **2009**, *79*, 195-205.

9. M.M. Logan, T. Toma, R. Thomas-Tran, J. Du Bois, Asymmetric synthesis of batrachotoxin: Enantiomeric toxins show functional divergence against Na_V. *Science* **2016**, *354*, 865-869.

10. W.A. Catterall, Voltage-Gated Sodium Channels at 60: Structure, Function, and Pathophysiology, *J. Physiol.* **2012**, *590*, 2577-2589.

11. (a) W.A Catterall, G. Wisedchaisri, N. Zheng, The chemical basis for electrical signaling. *Nat. Chem. Biol.* **2017**, *13*, 455-463. (b) F. Bezanilla, How membrane proteins sense voltage. *Nat. Rev. Mol. Cell Biol.* **2008**, *9*, 323-332.

12. J. Patlak, Molecular Kinetics of Voltage-Dependent Na^+ Channels. *Physiolog. Rev.* **1991**, *71*, 1047-1080.

13. J.W. West, D.E. Patton, T. Scheuer, Y. Wang, A.L. Goldin, W.A. Catterall, A Cluster of Hydrophobic Amino Acid Residues Required for Fast Na^+-Channel Inactivation, *Proc. Nat. Acad. Sci. USA* **1992**, *89*, 10910-10914.

14. X. Pan, Z. Li, Q. Zhou, H. Shen, K. Wu, X. Huang, J. Chen, J. Zhang, X. Zhu, J. Lei, W. Xiong, H. Gong, B. Xiao, N. Yan. Structure of the human voltage-gated sodium channel $Na_V1.4$ in complex with β1. *Science* **2108**, *362*, eaau2486.

15. (a) Y.Y. Vilin, P.C. Ruben, Slow Inactivation in Voltage-Gated Sodium Channels. *Cell Biochem. And Biophys.* **2001**, *35*, 171-190. (b) J. Silva, Slow Inactivation of Na^+ Channels, *Voltage Gated Sodium Channels*, Handbook of Experimental Pharmacology 221, Reuben, P. C., Ed., Springer-Verlag, Berlin, 2014, pgs 33-49.

16. (a) C.M. Armstrong, Na Channel Inactivation from Open and Closed States. *Proc. Nat. Acad. Sci. USA* **2006**, *103*, 17991-17996. (b) L. Goldman, Sodium Channel Inactivation from Closed States: Evidence for an Intrinsic Voltage Dependency. *Biophys. J.* **1995**, *69*, 2369-2377.

17. S. Wang, G.K. Wang, Voltage-Gated Sodium Channels as Primary Targets of Diverse Lipid-Soluble Neurotoxins. *Cell. Signal.* **2013**, *15*, 151-159.

18. (a) F. Märki, B. Witkop, The Venom of the Colombian Arrow Poison Frog *Phyllobates bicolor*. *Experientia* **1963**, *19*, 329-338. (b) J.W. Daly, B. Witkop, P. Bommer, K. Biemann, Batrachotoxin. The Active Principle of the Colombian Arrow Poison Frog. *J. Am. Chem. Soc.* **1965**, *87*, 124-126. (c) T. Tokuyama, J. Daly, B. Witkop, I.L. Karle, J. Karle, The Structure of Batrachotoxinin A, a Novel Steroidal Alkaloid from the Colombian Arrow Poison Frog. *J. Am. Chem. Soc.* **1968**, *90*, 1917-1918. (d) T. Tokuyama, J. Daly, B. Witkop, The Structure of Batrachotoxin, a Steroidal Alkaloid from the Colombian Arrow Poison Frog, *Phyllobates aurotaenia*, and Partial Synthesis of Batrachotoxin and its Analogs and Homologs. *J. Am. Chem. Soc.* **1969**, *91*, 3931-3938.

19. S.Y. Wang, J. Mitchell, D.B. Tikhonov, B.S. Zhorov, G.K Wang, How Batrachotoxin Modifies the Sodium Channel Permeation Pathway: Computer Modeling and Site-Directed Mutagenesis, *Mol. Pharmacol.* **2006**, *69*, 788-795.

20. (a) S.Y. Wang, G.K. Wang, Point Mutations in Segment I-S6 Render Voltage-Gated Na^+ Channels Resistant to Batrachotoxin. *Proc. Natl. Acad. Sci. USA.* **1998**, *95*, 2653-2658. (b) S.Y. Wang, G.K. Wang, Batrachotoxin-Resistant Na^+ Channels Derived from Point Mutations in Transmembrane Segment D4-S6. *Biophys. J.* **1999**, *76*, 3141-3149. (c) S.Y. Wang, C. Nau, G.K. Wang, Residues in Na^+ Channel D3-S6 Segment Modulate Both Batrachotoxin and Local Anesthetic Affinities. *Biophys. J.* **2000**, *79*, 1379-1387. (d) S.Y. Wang, M. Barile, G.K. Wang, Disparate Role of Na^+ Channel D2-S6 Residues in Batrachotoxin and Local Anesthetic Action. *Mol. Pharmacol.* **2001**, *59*, 1100-1107. (e) H. Li, D. Hadid, D.S. Ragsdale, The Batrachotoxin Receptor on the Voltage-Gated Sodium Channel is Guarded by the Channel Activation Gate. *Mol. Pharmacol.* **2002**, *61*, 905-912. (f) S.Y. Wang, D.B. Tikhonov, B.S. Zhorov, J. Mitchell, G.K. Wang, Serine-401 as a Batrachotoxin- and Local Anesthetic-Sensing Residue in the Human Cardiac Na^+ Channel. *Pflugers Arch.* **2007**, *454*, 277-287. (g) Y. Du, D.P. Garden, L. Wang, B.S. Zhorov, K. Dong, Identification of New Batrachotoxin-sensing Residues in Segment IIIS6 of the Sodium Channel *J. Biol. Chem.* **2011***, 286*, 13151-13160. (h) S.Y. Wang, G.K. Wang, Single Rat Muscle Na^+ Mutation Confers Batrachotoxin Autoresistance Found in Poison Dart Frog *Phyllobates terribilis*, *Proc. Nat. Acad. Sci. USA*, **2017**, *114*, 10491-10496.

21. E.X. Albuquerque, J.W. Daly, B. Witkop, Batrachotoxin: Chemistry and Pharmacology. *Science* **1971**, *172*, 995-1002.

22. D.B. Tikhonov, B.S. Zhorov, Sodium channel activators: Model of binding inside the pore and a possible mechanism of action. *FEBS Lett.* **2005**, *579*, 4207-4212.

23. cLogP values were calculated online using MolInspiration (www.molinspiration.com, 2018)

24. J. Tanguy, J.Z. Yeh, BTX modification of Na channels in squid axons, *J. Gen. Physiol.* **1991**, *97*, 499-519.

25. S. Bendahhou, T.R. Cummins, R. Tawil, S.G. Waxman, L.J. Ptácek, Activation and inactivation of the voltage-gated sodium channel: role of segment S5 revealed by a novel hyperkalaemic periodic paralysis mutation. *J. Neurosci.* **1999**, *19*, 4762-4761.

26. T.R. Cummins, J.R. Howe, S.G. Waxman, Slow Closed-State Inactivation: A Novel Mechanism Underlying Ramp Currents in Cells Expressing the hNE/PN1 Sodium Channel, *J. Neurosci.* **1998**, *18*, 9607-9619.

27. (a) G.K. Wang, S.-Y. Wang, Modification of Cloned Brain Na^+ Channels by Batrachotoxin, *Pflügers Arch.–Eur. J. Physiol.* **1994**, *427*, 309-316. (b) S.-Y. Wang, G.K. Wang, Slow Inactivation of Muscle μ1 Na^+ Channels in Permanently Transfected Mammalian Cells, *Pflügers Arch.–Eur. J. Physiol.* **1996**, *432*, 692-699.

28. (a) J. Payandeh, D.L. Minor Jr., Bacterial Voltage-Gated Sodium Channels ($BacNa_Vs$) from the Soil, Sea, and Salt Lakes Enlighten Molecular Mechanisms of Electrical Signaling and Pharmacology in the Brain and Heart, *J. Mol. Biol.* **2015**, *427*, 3-30. (b) J. Payandeh, Progress in understanding slow inactivation speeds up. *J. Gen. Physiol.* **2018**, *150*, 1235-1238.

29. M.J. Lenaeus, T.M. Gamal El-Din, C. Ing, K. Ramanadane, R. Pomès, N. Zheng, W.A. Catterall, Structures of closed and open states of a voltage-gated sodium channel. *Proc. Natl. Acad. Sci. USA* **2017**, *114*, E3051-E3060.

30. R.K. Finol-Urdaneta, J.R. McArthur, M.P. Goldschen-Ohm, R. Gaudet, D.B. Tikhonov, B.S. Zhorov, R.J. French, Batrachotoxin acts as a stent to hold open homotetrameric prokaryotic voltage-gated sodium channels. *J. Gen. Physiol.* **2019**, *151*, 186-199.

31. C. Arrigoni, A. Rohaim, D. Shaya, F. Findeisen, R.A. Stein, S.R. Nurva, S. Mishra, H.S. Mchaourab, D.L. Minor Jr., Unfolding of a Temperature-Sensitive Domain Control Voltage-Gated Channel Activation, *Cell* **2016**, *164*, 922-936.

32. D. Shaya, F. Findeisen, F. Abderemane-Ali, C. Arrigoni, S. Wong, S.R. Nurva, G. Loussouarn, D.L. Minor Jr., Structure of a Prokaryotic Sodium Channel Pore Reveals Essential Gating Elements and an Outer Ion Binding Site Common to Eukaryotic Channels, *J. Miol. Biol.* **2014**, *426*, 467-483.

33. (a) V. Vedantham, S.C. Cannon, Slow Inactivation Does Not Affect Movement of the Fast Inactivation Gate in Voltage-Gated Na^+ Channels, *J. Gen. Physiol.* **1998**, *111*, 83-93. (b) K. Hilber, W. Sandtner, O. Kudlacek, B. Schreiner, I. Glaaser, W. Schütz, H.A. Fozzard, S.C. Dudley, H. Todt, Interaction Between Fast and Ultra-Slow Inactivation in the Voltage-Gated Sodium Channel: Does the Inactivation Gate Stabilize the Channel Structure? *J. Biol. Chem.* **2002**, *277*, 37105-37115. (c) S.Y. Wang, K. Bonner, C. Russell, G.K. Wang, Tryptophan Scanning of DIS6 and D4S6 C-Termini in Voltage-Gated Sodium Channels, *Biophys. J.* **2003**, *85*, 911-920.

34. (a) Y.Y. Vilin, E. Fujimoto, P.C. Ruben, A Single Residue Differentiates between Human Cardiac and Skeletal Muscle Na^+ Channel Slow Inactivation, *Biophys. J.* **2001**, *80*, 2221-2230. (b) J. Webb, FF. Wu, S.C. Cannon, Slow Inactivation of the $Na_V1.4$ Sodium Channel in Mammalian Cells is Impeded by Co-expression of the β1 Subunit, *Pflügers Arch.–Eur. J. Physiol.* **2009**, *457*, 1253-1263.

35. (a) D.E. Featherstone, J.E. Richmond, P.C. Ruben, Interaction Between Fast and Slow Inactivation in Skm1 Sodium Channels, *Biophys. J.* **1996**, *71*, 3098-3109. (b) T.R. Cummins, F.J. Sigworth, Impaired Slow Inactivation in Mutant Sodium Channels, *Biophys. J.* **1996**, *71*, 227-236. (c) L.J. Hayward, R.H. Brown Jr., S.C. Cannon, Slow Inactivation Differs Among Mutant Na Channels Associated with Myotonia and Periodic Paralysis, *Biophys. J.* **1997**, *72*, 1204-1219.

36. For a recent, comprehensive discussion on Na_V gating, see: W.A Catterall, G. Wisedchaisri, N. Zheng, The conformational cycle of a prototypical voltage-gated sodium channel, *Nat. Chem. Biol.* **2020**, *16*, 1314-1320.

37. B.I. Khodorov, E.A. Yelin, L.D. Zaborovskaya, M.Z. Maksudov, O.B. Tikhomirova, V.N. Leonov, Comparative Analysis of the Effects of Synthetic Derivatives of Batrachotoxin on Sodium Currents in Frog Node of Ranvier, *Cell. Mol. Neurobiol.* **1992**, *12*, 59-81.

38. S.R. Schow, D.P. Rossignol, A.E. Lund, M.E. Schnee, Batrachotoxin Binding Site Antagonists, *Bioorg. Med. Chem. Lett.* **1997**, *7*, 181-186.

39. T. Toma, M.M. Logan, F. Menard, A.S. Devlin, J. Du Bois, Inhibition of Sodium Ion Channel Function with Truncated Forms of Batrachotoxin, *ACS Chem. Neurosci.* **2016**, *7*, 1463-1468.

40. B.M. Andresen, J. Du Bois, De Novo Synthesis of Modified Saxitoxins for Sodium Ion Channel Study. *J. Am. Chem. Soc.* **2009**, *131*, 12524-12525.

41. O. Moran, A. Picollo, F. Conti, Tonic and Phasic Guanidinium Toxin-Block of Skeletal Muscle Na Channels Expressed in Mammalian Cells. *Biophys. J.* **2003**, *84*, 2999-3006.